Journal of Solid State Chemistry **163,** 449–454 (2002)
doi:10.1006/jssc.2001.9424, available online at http://www.idealibrary.com on IDEAL®

Synthesis and Structure of $Ba_8Cu_3In_4N_5$ with Nitridocuprate Groups and One-Dimensional Infinite Indium Clusters

Hisanori Yamane,[1] Shinya Sasaki, Shun-ichi Kubota, Ryo Inoue, and Masahiko Shimada

Institute of Multidisciplinary Research for Advanced Materials, Tohoku University, 2-1-1 Katahira, Aoba-ku, Sendai 980-8577, Japan

and

Takashi Kajiwara

Department of Chemistry, Graduate School of Science, Tohoku University, Aramaki, Aoba-ku, Sendai 980-8577, Japan

Received June 8, 2001; in revised form October 2, 2001; accepted October 5, 2001

Single crystals of the quaternary compound $Ba_8Cu_3In_4N_5$ were prepared by heating Ba, Cu, and In in a Na flux at 1023 K under 7 MPa of N_2, and by slow cooling from this temperature. The crystal structure was analyzed by single-crystal X-ray diffraction. It crystallizes in an orthorhombic cell (space group *Immm* (No. 71), $Z = 2$) with $a = 4.0781(6)$, $b = 12.588(2)$, and $c = 19.804(3)$ Å at 298 K. The structural formula is expressed as $Ba_8[CuN_2]_2[CuN]In_4$. Nitridocuprates of one-dimensional chains $^1_\infty[CuN_{2/2}]$ and isolated units $^0[CuN_2]$, and one-dimensional indium clusters $^1_\infty[In_2In_{4/2}]$ are contained in the structure. A split-site model applied for the arrangement of $^1_\infty[CuN_{2/2}]$ chains suggested that there is a short-bond, long-bond alternation of the Cu–N bondings. The electrical resistivity of $Ba_8Cu_3In_4N_5$ was 3.44 mΩ · cm at 298 K. A metallic temperature dependence of the resistivity was observed down to 10 K. © 2002 Elsevier Science (USA)

Key Words: **barium copper nitride indium; crystal structure; single-crystal X-ray diffraction; nitridocuprates; Zintl anion; indium cluster.**

INTRODUCTION

For the past decade, many new *AE*–*M*–N ternary nitrides ($AE_xM_yN_z$, *AE* = Ba, Sr, and Ca, *M* = Fe, Ni, Co, Cu, Zn, Ga, etc.) have been synthesized and their structures were determined by X-ray diffraction (1, 2). In these ternary nitrides, electrons are transferred from electropositive alkaline-earth atoms to form various kinds of nitridometallate anions with isolated, or one-, two-, or three-dimensional extended structures. These anions often adopt structures that are isostructural with isoelectronic molecules or polyanions of main group elements. In some cases, Zintl anions were found in ternary compounds containing nitrogen, such as one-dimensional zigzag chain $^1_\infty$[In] in Ca_4In_2N and Sr_4In_2N (3) and $^1_\infty$[Ge] in $Ba_3Ge_2N_2$ (4), and trigonal bipyramids of $^0[Ga_5]$ in Sr_6Ga_5N and Ba_6Ga_5N (5).

The difficulty in preparing ternary copper nitrides was pointed out because copper nitride Cu_3N decomposes at 743 K to copper and nitrogen (6, 7). Recently, some new ternary and quaternary nitrides containing alkaline-earth metals and copper, $Sr_6Cu_3N_5$, SrCuN (8), BaCuN, $Ba_{16}Cu_{13}N_{15}$, and $Ca_4BaCu_2N_4$ (9), as well as other ternary compounds (1, 2), were synthesized in sodium fluxes under medium nitrogen pressure. In the present study, single crystals of a new quaternary compound $Ba_8Cu_3In_4N_5$ containing nitridometallate anions and one-dimensional infinite Zintl clusters were synthesized by using the Na flux method. We report the preparation, crystal structure, and electrical resistivity of this compound.

EXPERIMENTAL

All manipulations were carried out in an Ar-filled glove box. Ba (Aldrich, 99.99%), Cu (High Purity Chemical, 99.99%), In (Rare Metallic, 99.999%) and Na (High Purity Chemical, 99%) were used as starting materials. Ba (0.465 mg), Cu (0.108 mg), In (0.194 mg), and Na (0.234 mg) with a Ba:Cu:In:Na molar ratio of 2:1:1:6 were weighed and put into a BN crucible (inside diameter 7 mm, height 37.5 mm). The crucible was placed into a stainless-steel container and sealed in the glove box. The container was made of a stainless-steel tube ($\frac{1}{2}$ inch outer diameter, 1 mm thick), a stainless steel seal cap, a valve, and a pressure gage. A schematic illustration of the stainless-steel container was shown in our previous paper (10). The container was

[1]To whom correspondence should be addressed. Fax: 81-22-217-5160. E-mail: yamane@tagen.tohoku.ac.jp.

0022-4596/02 $35.00

connected to a N_2 gas feed line. After heating to 1023 K in an electric furnace, N_2 gas (Nippon Sanso, $> 99.9999\%$) was introduced into the container and the pressure was maintained at 7 MPa with a pressure regulator. The sample was heated at this temperature for 1 h and then cooled from 1023 to 823 K at a rate of 2 K/h under 7 MPa of N_2. Below 823 K, the sample was cooled to room temperature by shutting off the electric power to the furnace. The products in the crucible were washed in liquid NH_3 (Nippon Sanso, 99.999%) to dissolve away the Na flux. The details of the Na extraction procedure were described previously (11).

Characteristic X-ray spectra of Ba, In, and Cu in the crystals were measured by energy dispersive X-ray spectroscopy (Voyger EDX) on a scanning electron microscope (Jeol ISM-5400). The molar ratio of these elements was obtained by quantitative analysis of the spectra using the attached software without a standard sample. The nitrogen content in the compound was determined from the results of ion chromatography. The crystals were dissolved in 0.04 N sulfuric acid solution to capture the N as NH_4^+, undissolved products such as $BaSO_4$ were filtered, and the concentration of NH_4^+ ion in the solution was analyzed with an ion chromatographic analyzer (Toa ICA-3000).

Since the single crystals were not stable in the air, crystals for X-ray diffraction study were sealed in glass capillaries. Precession photographs were taken using Mo$K\alpha$ radiation. X-ray diffraction intensity data were collected at 298 K using a single-crystal X-ray diffractometer with a two-dimensional CCD detector (Bruker SMART System). The unit cells were refined during the integration with the program SAINT (12). A face-indexed analytical absorption correction was applied to the collected diffraction intensity data with the program XPREP (13). A structure model was obtained by the direct method with the program SIR97 (14). Refinement was performed using SHELXL97 (15). Fourier analysis was carried out with the program JANA2000 (16).

The electrical resistivity of a single crystal with a size of $3.0 \times 0.6 \times 0.5\ mm^3$ was measured in an Ar gas-filled cell from about 10 K to room temperature by a direct-current four-probe method using In as electrodes.

RESULTS AND DISCUSSION

Thin prismatic single crystals with a black metallic luster (maximum size, $4–5 \times 1.0 \times 0.5\ mm^3$) were obtained in the reaction product. The Ba:Cu:In molar ratio obtained by EDX analysis for three different single crystals was in the range of 7.9–8.3:2.7–3.1:4, and agreed well with the ideal molar ratio from the formula of $Ba_8Cu_3In_4N_5$. The nitrogen content determined by ion chromatography with 27.5 mg of the single crystals was 3.9 wt% which was identical to the value (3.9 wt%) calculated from the formula.

Table 1 summarizes the results of the X-ray diffraction experiments. Precession photographs showed that this compound crystallizes with an orthorhombic body-centered lattice ($a = 4.08$, $b = 12.59$, and $c = 19.80$ Å). The long dimension of the single crystals was parallel to the a axis. Four possible space groups, $I222$, $I2_12_12_1$, $Imm2$, and $Immm$, are consistent with the observed systematic extinctions. Crystal structure refinement based on a model from the direct method was performed using the highest symmetry group $Immm$ with $R1$ of 3.30% and $wR2$ of 8.71%. The structure model is composed of isolated nitridocuprates $^0[CuN_2]$ of [N1–Cu1–N1], one-dimensional infinite chains $^1_\infty[CuN_{2/2}]$ of [–Cu2–N2–], and one-dimensional infinite clusters $^1_\infty[In_2In_{4/2}]$ of [–$(In1)_2$– $(In2)_2$–]. However, values of principal mean square atomic displacements, U_{11}, were large for Cu2 at the position of (0.5, 0, 0), 0.136(4) $Å^2$, and for N2 (0, 0, 0), 0.15(3)$Å^2$. Since two peaks were clearly seen on the a–b plane along the a axis and near the position of N2 in the Fourier map, we applied a split-site model to the Cu2 and N2 sites.

When the isotropic displacement parameters were changed into anisotropic ones simultaneously during the refinement, some parameters of the principal axes for the Cu2 and N2 sites went to negative values. Thus, we changed the values step by step, first for the Cu2 site and then for the

TABLE 1
Crystal Data and Structure Refinement for $Ba_8Cu_3In_4N_5$

Formula	$Ba_8Cu_3In_4N_5$
Formula weight	1818.67
Crystal size	$0.30 \times 0.20 \times 0.08$ mm
Temperature	298(2) K
Crystal system, space group	Orthorhombic, *Immm*
Unit cell dimensions	$a = 4.0781(6)$ Å $b = 12.588(2)$ Å $c = 19.804(3)$ Å
Volume	1016.7(2) $Å^3$
Z, Calculated density	2, 5.941 Mg/m^3
Absorption coefficient	22.693 mm^{-1}
Theta range for data collection	1.92 to 30.02°
Limiting indices	$-5 \le h \le 4$, $-17 \le k \le 15$ $-27 \le l \le 27$
Reflections collected/unique	4383/898 [R (int)[a] = 0.0670]
Data/restrains/parameters	898/0/40
Goodness-of-fit S on F^2 [a]	1.099
Final R indices [$I > 2\sigma(I)$][a]	$R1 = 0.0326$, $wR\ 2 = 0.0846$
R indices (all data)[a]	$R1 = 0.0339$, $wR\ 2 = 0.0854$
Extinction coefficient	0.0052(3)
Largest diff. peak and hole	2.175 and -3.705 e.$Å^{-3}$

[a] R (int) $= \sum|\mathrm{av}\Delta(I)|/\sum|\mathrm{av}(I)|$, the residual for symmetry-equivalent reflections, where av (I) is the average intensity and $\Delta(I)$ is the average difference between av(I) and the individual intensities. $R1 = \sum||F_o| - |F_c||/\sum|F_o|$, $wR2 = [\sum w(F_o^2 - F_c^2)^2/\sum(wF_o^2)^2]^{1/2}$, $w = 1/[\sigma^2(F_o^2) + (0.0419P)^2 + 18.51P]$, where F_o is the observed structure factor, F_c is the observed structure factor, σ is the standared deviation of F_c^2, and $P = [\mathrm{Max}(F_o^2, 0) + 2F_c^2]/3$.

$S = [\sum w(F_o^2 - F_c^2)^2/(n-p)]^{1/2}$, where n is the number of reflectons and p is the total number of parameters refined.

TABLE 2
Atomic Coordinates and Isotropic Displace Parameters of $Ba_8Cu_3In_4N_5$

Atom	Site	Occ.	x	y	z	U_{eq}[a]
Ba1	8*l*	1.0	0.5	0.3550(1)	0.2081(1)	13(1)
Ba2	8*l*	1.0	0.5	0.3438(1)	0.4038(1)	17(1)
In1	4*h*	1.0	0.5	0.6310(1)	0	28(1)
In2	4*j*	1.0	0	0.5	0.0802(1)	25(1)
Cu1	4*j*	1.0	0.5	0	0.1918(1)	13(1)
Cu2	4*e*	0.5	0.446(4)	0	0	43(3)
N1	8*l*	1.0	0	0.3507(5)	0.3058(3)	16(1)
N2	4*e*	0.5	0.083(6)	0	0	35(7)

[a] The equivalent isotropic displacement parameter, U_{eq} in $Å \times 10^3$, is defined as one-third of the trace of the orthogonalized U_{ij} tensor.

N2 site. The atomic parameters and anisotropic displacement parameters refined with the split-site model are shown in Tables 2 and 3, respectively. The R values decreased to $R1 = 3.26$, $wR2 = 8.46\%$. Although the distances between the split sites are small (Cu2–Cu2, 0.44 Å and N2–N2, 0.67 Å), SHELXL97 refined the anisotropic parameters with smaller values of U_{11} (Cu2, 0.075(10) $Å^2$ and N2, 0.05(2) $Å^2$). The deepest hole of -3.71 e/$Å^3$ was observed at (0, 0.4839, 0.4813), which is between the two split Cu2 sites with a distance of 0.48 Å from Cu2.

We also examined an ordered structure model with a lower symmetry space group *I2mm*. The structure was refined with $R1 = 3.72$, $wR2 = 9.75\%$, and Flack parameter of 0.2(2) (17). The refined atomic parameters of Cu2 and N2 were (0.479(4), 0, 0) and (0.072(5), 0, 0), respectively. However, the U_{11} displacement parameter of Cu2 was still large (0.130(4) $Å^2$). We could not refine a split-site model at the Cu2 site with this space group because the displacement parameters diverged from reasonable values during the refinement. We also tried the twin option in the SHELXL97 program, but did not see any improvement. A small peak was observed between Cu2 and N2 on the Fourier map calculated with the ordered model. The peak position was close to another N2 position in the split-site model of *Immm*. Therefore, we chose the split-site model of *Immm* as a better model to explain the diffraction data. Figure 1 illustrates the arrangement of atomic positions along the *a*–*b* plane (a) and the *b*–*c* plane (b) with displacement ellipsoids. Table 4 lists selected interatomic distances and bond angles.

In the precession photograph taken with longer exposure time, we could not see any reflections from a superlattice. We also collected the X-ray diffraction data at 173 K. The

TABLE 3
Anisotropic Displacement Parameters ($Å^2 \times 10^3$) for $Ba_8Cu_3In_4N_5$[a]

Atom	U_{11}	U_{22}	U_{33}	U_{23}	U_{13}	U_{12}
Ba(1)	14(1)	10(1)	16(1)	1(1)	0	0
Ba(2)	20(1)	16(1)	15(1)	0(1)	0	0
In(1)	37(1)	15(1)	32(1)	0	0	0
In(2)	31(1)	29(1)	16(1)	0	0	0
Cu(1)	13(1)	8(1)	17(1)	0	0	0
Cu(2)	75(10)	28(2)	27(1)	0	0	0
N(1)	19(3)	10(3)	20(3)	1(2)	0	0
N(2)	50(20)	37(12)	20(9)	0	0	0

[a] The anisotropic displacement factor exponent takes the form $-2\pi^2[h^2a^{*2}U_{11} + \cdots + 2hka^*b^*U_{12}]$.

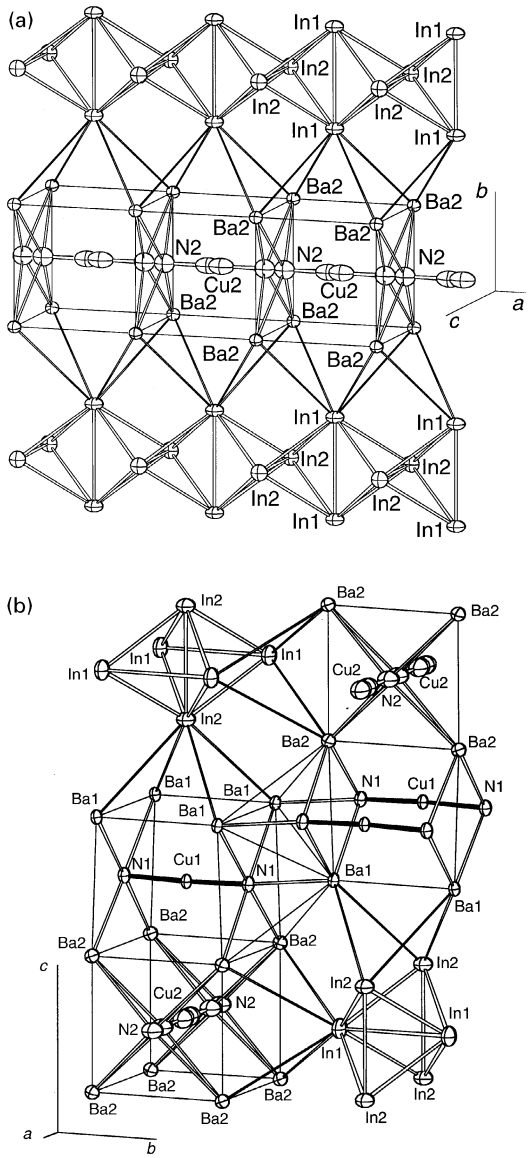

FIG. 1. Arrangement of atomic positions in the $Ba_8Cu_3In_4N_5$ structure illustrated with 50% probability displacement ellipsoids at sections along the *a*–*b* plane ($x = -1.2$ to $+2.7$, $y = -0.7$ to $+0.7$, $z = -0.1$ to $+0.1$) (a) and the *b*–*c* plane ($x = -0.25$ to $+1.25$, $y = -0.25$ to $+0.75$, $z = -0.1$ to $+0.6$) (b).

TABLE 4
Selected Interatomic Distances (Å) and Bond Angles (°) for $Ba_8Cu_3In_4N_5$

Ba1–N1	2.604(7)	In1–Ba2	3.8687(9)
Ba1–N1	2.811(5)	In2–Ba1	3.7295(9)
Ba1–Ba1	3.6497(10)	Cu1–N1	1.880(7)
Ba1–Ba1	3.7286(8)	Cu1–Ba1	3.3783(9)
Ba1–Ba2	3.8778(8)	Cu1–Ba2	3.4074(9)
Ba1–Ba2	3.9163(7)	Cu2–N2	1.92(3)
Ba2–N2	2.758(3)	Cu2–N2	2.15(3)
Ba2–N1	2.816(5)	Cu2–Ba2	3.286(8)
Ba2–Ba2	3.8105(11)	Cu2–Ba2	3.551(10)
Ba2–Ba2	3.9321(10)	N1–Cu1–N1	177.2(4)
In1–In2	3.0655(8)	N2–Cu2–N2	180.0
In1–In1	3.298(2)	Cu2–N2–Cu2	180.0
In2–In2	3.175(2)		

lattice parameters were 0.11% smaller along the *a* and *b* axes, and 0.24% smaller along the *c* axis than those at 298 K. However, no significant change was observed by the structure refinement with the low-temperature data.

A model with split atomic positions of Ni and N was presented for the structure analysis of Sr_2NiN_2 to explain the subcell of a superstructure (18). The split sites were placed along the axis of an isolated linear nitridometallate anion $^0[NiN_2]^{4-}$ of [N–Ni–N]. Based on the Na_2HgO_2 structure, the same bond length of 1.8 Å was selected for both sides of Ni–N bonds. Since a superstructure lattice was ascertained by X-ray precession photographs and X-ray powder diffraction, a superstructure model was proposed with the displacement of the [N–Ni–N] units.

In the case of $^1_\infty[CuN_{2/2}]$ infinite chain in $Ba_8Cu_3In_4N_5$, a possible arrangement of Cu2 and N2 sites on the *a* axis is short-bond, long-bond alternation with distances of 1.92(3) and 2.15(3) Å. The other set of the distances does not seem to be realistic due to the very short Cu–N distance of 1.48(3) Å. The N2 site of the [–Cu2–N2–] infinite chain is surrounded by four equivalent Ba2 atoms with a Ba2–N2 distance of 2.758(3) Å. Because large anisotropy is not seen for Ba2 and other nonsplit atoms and the $^1_\infty[CuN_{2/2}]$ chains are 11.73 Å apart from each other in the crystal structure, the $^1_\infty[CuN_{2/2}]$ chains could take their positions independently in the rectangular column of Ba2 atoms along the *a* axis (Fig. 1a). This disorder arrangement of the $^1_\infty[CuN_{2/2}]$ chains with alternating long and short distances along the chain, as well as other possibilities of superstructures and twin or microdomain structures, may explain the statistical distribution at the split sites in the unit cell.

Nitridometallate infinite chains have been observed in the structures of Ca[CuN] with a Cu–N distance of 1.86 Å (19) and Ca[NiN] with a Ni–N distance of 1.7904 Å (20). Structures of Sr[CuN] (8), Ba[CuN] and $Ba_{16}[(CuN)_8][Cu_2N_3][Cu_3N_4]$ (9) also contain infinite chains of $^1_\infty[CuN_{2/2}]$ in which the copper atoms are almost linearly coordinated by nitrogen atoms. However, the chains kink at the third nitrogen atom for Sr[CuN] (zigzag chain), at the second nitrogen atom for Ba[CuN] (zigzag chain), and at the fist nitrogen atom for $Ba_{16}[(CuN)_8][Cu_2N_3][Cu_3N_4]$ (helix chain), with a bond angle of either about 90° or 180° at the nitrogen atoms. An alternated distortion of bond lengths in infinite one-dimensional structures is observed in some oxides and other inorganic and organic compounds, which is known as Piers distortion (21). Such kinds of distortion in the one-dimensional structure have not been reported for nitridocuprates and other nitridometallates.

The bond-length distortion of the linear infinite [–Cu2–N2–] chain could be explained by precise electron band structure calculation. From the crystallographic point of view, the distortion might be derived from a template effect of the one-dimensional indium clusters $^1_\infty[In_2In_{4/2}]$ situated on both sides of the $^1_\infty[CuN_{2/2}]$ chain (Fig. 1a). The periodicity of the lattice along the *a* axis is governed by the unit length of $^1_\infty[In_2In_{4/2}]$ clusters and the distance between Cu2 and N2 might be expanded. In order to reduce the instability by the elongation of bonding, alternating bong-length distortion could occur. If $^1_\infty[In_2In_{4/2}]$ clusters were not so rigid, the Cu2–N2 chain would be kinked as observed in the structures of Ba[CuN] and $Ba_{16}[(CuN)_8][Cu_2N_3][Cu_3N_4]$.

The distances of Cu2–N2 (1.92(3) and 2.15(3) Å, average 2.04 Å) of $Ba_8Cu_3In_4N_5$ are longer than the Cu(I)–N distances in $^1_\infty[CuN^{2-}_{2/2}]$ of Ca[CuN], Sr[CuN], Ba[CuN], and $Ba_{16}[(CuN)_8][Cu_2N_3][Cu_3N_4]$ (1.86–1.89 Å), and the Cu(I)–N bond length of two-fold-coordinated isolated group of $^0[CuN_2]^{5-}$ (1.86–1.87 Å) in $Sr_6[Cu_2N_3][CuN_2]$ and $Ca_4Ba[CuN_2]_2$. However, the distance of 1.92(3) Å is close to distances observed between Cu(I) and N atoms at a kink position in a Z-shaped group $^0[Cu_3N_4]^{9-}$ (1.93(6) Å) and in the helix chain $^1_\infty[CuN^{2-}_{2/2}]$ (1.91(3) Å) in $Ba_{16}[(CuN)_8][Cu_2N_3][Cu_3N_4]$, and in a V-shaped group of $[Cu_2N_3]^{7-}$ (1.93(2) Å) in $Sr_6[Cu_2N_3][CuN_2]$. The distance of 2.15(3) Å is larger than these Cu–N distances, but close to that of 2.08(4) Å reported for two-fold linear-coordinated Cu(I) in $CuTaN_2$ which was prepared by exchange reaction of $NaTaN_2$ with CuI at 673 K (7).

Bond valence sums calculated with the bond-valence parameter ($R_{Cu-N} = 1.61$ Å) proposed by Brese and O'Keeffe (22) are 0.84–0.99 for Cu atoms in Ca[CuN], Sr[CuN], Ba[CuN], $Sr_6[Cu_2N_3][CuN_2]$, $Ba_{16}[(CuN)_8][Cu_2N_3][Cu_3N_4]$, and $Ca_4Ba[CuN_2]_2$, confirming the formal valence state of Cu(I). On the other hand, the bond valence sums are 0.66 for Cu2 atoms in $Ba_8Cu_3In_4N_5$, and 0.56 for $Cu(I)TaN_2$.

The Cu1 atom is almost linearly coordinated by two N1 atoms ($\angle$ N1–Cu1–N1 = 177.2(4)°), forming an isolated nitridocuprate group $^0[CuN_2]$. Similar [N–Cu–N] units are contained in the structures of $Sr_6[Cu_2N_3][CuN_2]$ and $CaBa[CuN_2]_2$. The Cu1–N1 bond distance of 1.880(7) Å is

comparable with the Cu–N distances of 1.86(2) Å and 1.865(5) Å in $^0[CuN_2]^{5-}$ of $Sr_6[Cu_2N_3][CuN_2]$ and $CaBa[CuN_2]_2$, respectively. The bond valence sum calculated for Cu1 is 0.96, indicating Cu(I) valence and formal charge of -5 for the isolated group of $^0[CuN_2]$. The $^0[CuN_2]^{5-}$ anion has the same valence electron count as CO_2, since the number of all electrons without closed *d*-orbital electrons is 16.

The [N1–Cu1–N1] units align along the *b* axis direction and perpendicular to the [–Cu2–N2–] chain (Fig. 1b). The N1 atom is surrounded by two Ba1 atoms with a distance of 2.811(5) Å and by two Ba2 atoms with a distance of 2.816(5) Å. Another Ba1 atom is located 2.604(7) Å from the N1 atom along the *b* axis and at the other side of Cu1 atom. This distance is close to the shortest Ba–N distance (2.64(3) Å) observed in $Ba_{16}[(CuN)_8][Cu_2N_3][Cu_3N_4]$. While Ba1–Ba1 and Ba2–Ba2 sites align with the period of the *a* axis length (4.0781(6) Å), the Ba1–Ba1 distance of 3.6497(10) Å is shorter than the Ba2–Ba2 of 3.9321(10) Å along the *b* axis direction. The [N1–Cu1–N1] unit bends toward the side of Ba2 atoms.

As illustrated in Fig. 1, tetrahedra of In1 and In2 atoms share edges and form a one-dimensional In cluster $^1_\infty[In_2In_{4/2}]$. Similar arrangements of In tetrahedra can be seen in part along the *c* axis of the tetragonal structure of In metal, although all edges are shared with the next four rows of In tetrahedra. The distances between In1–In1 and In2–In2 atoms on the shared edges are 3.298(2) and 3.176(2) Å, respectively. The length of unshared In1–In2 edges is 3.0655(9) Å. These distances are comparable with the In–In distances of the isolated In tetrahedron in Na_2In (3.068(1), 3.127(2), and 3.152(1) Å) (23). The similar In–In interatomic distances have also been reported for other Zintl compounds of NaIn, $SrIn_2$, and $BaIn_2$ (2.97–3.28 Å) (24–26), and for In metal (3.24–3.38 Å) (27). The In1 and In2 are, respectively, equidistant to four equivalent Ba2 (3.8687(9) Å) and to four equivalent Ba1 (3.7295(9) Å). These distances are in the range of 3.54–3.88 Å reported for In–Ba distances in $BaIn_2$ (25).

The formal charge of In1 and In2 in $^1_\infty[In_2In_{4/2}]$ is simply estimated to be -1 from the formal charge of -2 for In in Na_2In with the isolated tetrahedron $^0[In_4]$. In^- ions in the Zintl compounds of NaIn, $SrIn_2$, and $BaIn_2$ are isoelectric with group IV tin and form three-dimensional four-connected net structures. The In^- ions in these structure are part of a distorted tetrahedron of neighbor In^- ions (26). The five bonds observed in the one-dimensional cluster of $^1_\infty[In_2In_{4/2}]$ cannot be explained by classical two-center two-electron valence rules. If the formal charges of Ba, N, and In atoms are $+2$, -3, and -1 respectively, and Cu1 in $^0[CuN_2]^{5-}$ is $+1$, $Ba_8Cu_3In_4N_5$ can be represented as $(Ba^{2+})_8(^0[CuN_2]^{5-})_2{}^1_\infty[CuN^{2-}_{2/2}]$ ($^1_\infty[In_2In^{4-}_{4/2}]$). The formal valence of Cu2 in $^1_\infty[CuN^{2-}_{2/2}]$ is I.

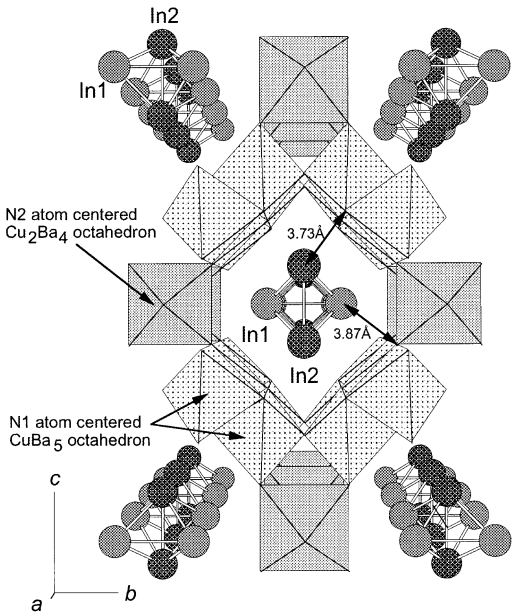

FIG. 2. Crystal structure of $Ba_8Cu_3In_4N_5$ shown in a representation using nitrogen-centered Ba and Cu polyhedra and $^1_\infty[In_2In_{4/2}]$ clusters.

Figure 2 illustrates the crystal structure of $Ba_8Cu_3In_4N_5$ with nitrogen-centered octahedra of Ba and Cu atoms. N1 atom-centered $(Ba1)_3(Ba2)_2Cu1$ octahedra share Ba1–Ba1 and Ba1–Ba2 edges and continue along the *a* axis. The arrays of the octahedra also connect to each other by sharing apical Cu1 atoms. N2 atom-centered $(Ba2)_4(Cu2)_2$ octahedra line along the *a* axis by sharing apical Cu2 atoms and connect to $(Ba1)_3(Ba2)_2Cu1$ octahedra by sharing Ba2 atoms. These nitrogen-centered octahedra construct channels along the *a* axis. The inner faces of the channel are planes of Ba atoms. One-dimensional In clusters of $^1_\infty[In_2In_{4/2}]$ are situated in these channels.

The temperature dependence of the electrical resistivity was measured along the elongated (*a* axis) direction of the single crystal. As shown in Fig. 3, electrical resistivity at 276 K was about 3.4 $m\Omega \cdot cm$ and decreased with decreasing temperature. However, the overall decrease is small and the resistivity at 10 K was about 2.3 $m\Omega \cdot cm$. A 5*s*–5*p* band of $^1_\infty[In_2In_{4/2}]$ seems most likely responsible for the metallic conduction. Molecular orbital calculations may help explain the conduction as well as the chemical bonding in $Ba_8Cu_3In_4N_5$.

To summarize, a new compound $Ba_8Cu_3In_4N_5$ which consists of nitridocupurate anions of $^0[CuN_2]^{5-}$ and $^1_\infty[CuN^{2-}_{2/2}]$ and a polyanion of $^1_\infty[In_2In^{4-}_{4/2}]$ were prepared using a Na flux. In the quaternary compounds, we think this is probably one of the rare examples that includes both nitridometallate anions and Zintl anions. Wide varieties of such new quaternary compounds and multicomponent compounds may be found in the future.

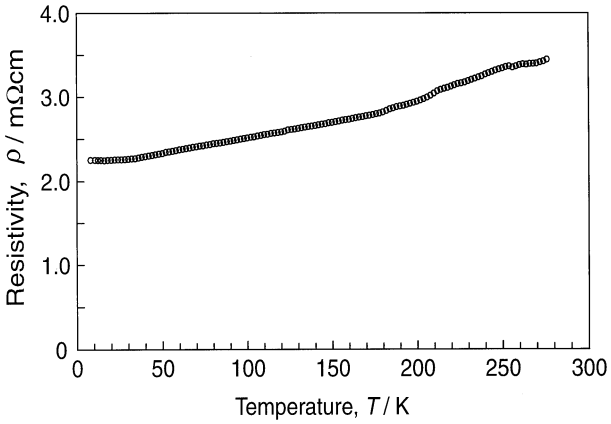

FIG. 3. Temperature dependence of electrical resistivity for $Ba_8Cu_3In_4N_5$.

ACKNOWLEDGMENTS

We thank Professor T. Ito for his encouragement and support and Y. Hayasaka for the EDX analysis. Useful discussions with F. J. DiSalvo (Cornell Univ.) are appreciated. G. Kowach and Z. Gal are acknowledged for helpful discussions and Fourier map calculations. This work was supported in part by the NEDO International Joint Research Program, and by a grant from the Ministry of Education, Culture, Sports, Science and Technology.

REFERENCES

1. F. J. DiSalvo and S. J. Clarke, *Curr. Opin. Solid State Mater. Sci.* **1,** 241–249 (1996).
2. R. Niewa and F. J. DiSalvo, *Chem. Mater.* **10,** 2733–2752 (1998).
3. G. Cordier and S. Rönninger, *Z. Naturforsh.* **42b,** 825–827 (1987).
4. H. Yamane and F. J. DiSalvo, *J. Alloys Compd.* **241,** 69–74 (1996).
5. G. Cordier, M. Ludwig, D. Stahl, P. C. Schmidt, and R. Kniep, *Angew. Chem., Int. Ed. Engl.* **34,** 1761–1763 (1995).
6. U. Zachwieja and H. Jacobs, *J. Less-Common Met.* **161,** 175–184 (1990).
7. U. Zachwieja and H. Jacobs, *Eur. J. Solid State Inorg. Chem.* **28,** 1055–1062 (1991).
8. F. J. DiSalvo, S. S. Trail, H. Yamane, and N. E. Brese, *J. Alloys Compd.* **255,** 122–129 (1997).
9. R. Niewa and F. J. DiSalvo, *J. Alloys Compd.* **279,** 153–160 (1998).
10. M. Aoki, H. Yamane, M. Shimada, T. Sekiguchi, T. Hanada, T. Yao, S. Sarayama, and F. J. DiSalvo, *J. Crystal Growth* **218,** 7–12 (2000).
11. G. R. Kowach, H. Y. Lin, and F. J. DiSalvo, *J. Solid State Chem.* **141,** 1–9 (1998).
12. Bruker, SAINT, Bruker AXS Inc., Madison, WI, 1997.
13. Bruker, XPREP, Bruker AXS Inc., Madison, WI, 1997.
14. A. Altomare, G. Cascarano, C. Giacovazzo, A. Guagliardi, M. C. Burla, G. Polidori, and M. Camalli, *J. Appl. Cryst.* **27,** 435 (1994).
15. G. M. Sheldrick, SHELXL97, University of Göttingen, Germany, 1997.
16. V. Petricek and M. Dusek, The crystallographic computing system JANA2000, Institute of Physics, Praha, Czech Republic, 2000.
17. H. D. Flack, *Acta Crystallogr. A* **39,** 876–881 (1983).
18. G. R. Kowach, N. E. Brese, U. M. Bolle, C. J. Warren, and F. J. DiSalvo, *J. Solid State Chem.* **154,** 542–550 (2000).
19. J. Jäger, Ph.D. Thesis, Technische Hochschule Darmstadt, 1995.
20. M. Y. Chern and F. J. DiSalvo, *J. Solid State Chem.* **88,** 459–464 (1990).
21. S. Kagoshima, H. Nagasawa, and T. Sambongi, "One-Dimensional Conductors," Springer Ser. Solid-State Sci., Vol. 72. Springer, Berlin, 1988.
22. N. E. Brese and M. O'Keeffe, *Acta Crystallogr. B* **47,** 192–197 (1991).
23. S. C. Sevov and J. D. Corbett, *J. Solid State Chem.* **103,** 114–130 (1993).
24. A. Iandelli, *Z. Anorg. Allg. Chem.* **330,** 221–232 (1964).
25. G. Bruzzone and G. B. Bonino, *Atti Accad. Nat. Lincei* **48,** 235–241 (1970).
26. G. Nuspl, K. Polborn, J. Evers, G. A. Landrum, and R. Hoffmann, *Inorg. Chem.* **35,** 6922–6932 (1996).
27. P. Villars and L. D. Calvert, "Peason's Handbook of Crystallographic Data for Intermetallic Phases," 2nd Ed. The Materials Information Society, Materials Park, OH, 1991.